

A Kinetic and Mechanistic Study of the Amino Acid Catalyzed Aldol Condensation of Acetaldehyde in Aqueous and Salt Solutions

Barbara Nozière*[†] and Armando Córdoba*[‡]

Department of Meteorology and Department of Organic Chemistry, Stockholm University, SE-106 91 Stockholm, Sweden

Received: October 3, 2007; In Final Form: January 2, 2008

The amino acid catalyzed aldol condensation is of great interest in organic synthesis and natural environments such as atmospheric particles. However, kinetic and mechanistic information on these reactions is limited. In this work the kinetics of the aldol condensation of acetaldehyde in water and aqueous salt solutions (NaCl, CaCl₂, Na₂SO₄, MgSO₄) catalyzed by five amino acids (glycine, alanine, serine, arginine, and proline) at room temperature (295 ± 2 K) has been studied. Monitoring the formation of three products, crotonaldehyde, 2,4-hexadienal, and 2,4,6-octatrienal, by UV–vis absorption over 200–1100 nm revealed two distinct kinetic regimes: at low amino acid concentrations (in all cases, below 0.1 M), the overall reaction was first-order with respect to acetaldehyde and kinetically limited by the formation of the enamine intermediate. At larger amino acid concentrations (at least 0.3 M), the kinetics was second order and controlled by the C–C bond-forming step. The first-order rate constants increased linearly with amino acid concentration consistent with the enamine formation. Inorganic salts further accelerated the enamine formation according to their p*K*_b, plausibly by facilitating the iminium or enamine formation. The rate constant of the C–C bond-forming step varied with the square of amino acid concentration suggesting the involvement of two amino acid molecules. Thus, the reaction proceeded via a Mannich pathway. However, the contribution of an aldol pathway, first-order in amino acid, could not be excluded. Our results show that the rate constant for the self-condensation of acetaldehyde in aqueous atmospheric aerosols (up to 10 mM of amino acids) is identical to that in sulfuric acid 10–15 M (*k*¹ ~ 10⁻⁷–10⁻⁶ s⁻¹) clearly illustrating the potential importance of amino acid catalysis in natural environments. This work also demonstrates that under usual laboratory conditions and in natural environments aldol condensation is likely to be kinetically controlled by the enamine formation. Notably, kinetic investigations of the C–C bond-forming addition step would only be possible with high concentrations of amino acids.

Introduction

The asymmetric aldol reaction is an important method for forming carbon–carbon bonds.^{1,2} In nature, this reaction is catalyzed by aldolase enzymes, which, if they are of class I, employ chiral enamines as nucleophiles to achieve stereoselective addition between carbonyl compounds in buffered aqueous media.¹ Another approach for achieving highly stereoselective aldol reactions in synthesis is the use of amino acids and their derivatives as catalysts in organic solvent.^{3,4} Moreover, amino acids and oligopeptides can catalyze these reactions in mild and environmentally compatible media such as water and aqueous salt solutions.⁵ Amino acids are ubiquitous in natural environments at earth's surface⁶ and in atmospheric particles. In particular, their concentrations are enriched by several orders of magnitudes in rain droplets,^{7,8} fog droplets,^{9,10} and aerosols^{10,11} compared to oceans and other natural waters. In this context, the amino acid catalyzed oligomerization of acetaldehyde in water and ionic solutions was recently shown to be an efficient route to linear conjugated olefinic compounds in atmospheric aerosols.¹² This formation of light-absorbing compounds in particles that would be otherwise transparent to light

was found to be potentially important for the optical properties of the aerosols and their contribution to climate.

Kinetic information on the amino acid catalyzed aldol condensation is, however, limited. Our recent study¹² reports some rate constants for these reactions in aqueous and salts media. Some aspects of their mechanism have also been addressed by studying the aldol reaction catalyzed by secondary and primary amines,^{5b} which involves the same mechanism as the aldol condensation apart from the final dehydration step.¹³ The retroaldol reaction of the amino acid catalyzed asymmetric aldol reaction has also been investigated¹⁴ and has been concluded to involve only one molecule of amino acid in the transition state.¹⁵ Solvent effects have also been studied for the initial steps of the amino acid catalyzed aldol reaction in organic media,^{13b,c} but the mechanisms affecting the rates of reaction could not be clearly identified. Thus, essential information on the mechanism of the amino acid catalyzed aldol condensation remains to be established, such as the reaction order in carbonyl compound, the identity of the step kinetically controlling the reaction (thus catalytic efficiency), and the reaction order in amino acid. Admittedly, a challenge encountered by previous studies was that they focused on cross-reactions, making it difficult to distinguish between the C–C bond-forming step from other steps (see mechanism below) on the basis of reaction order.

* Corresponding authors. E-mail: barbara.noziere@misu.su.se (B.N.); acordova@organ.su.se (A.C.).

[†] Department of Meteorology.

[‡] Department of Organic Chemistry.

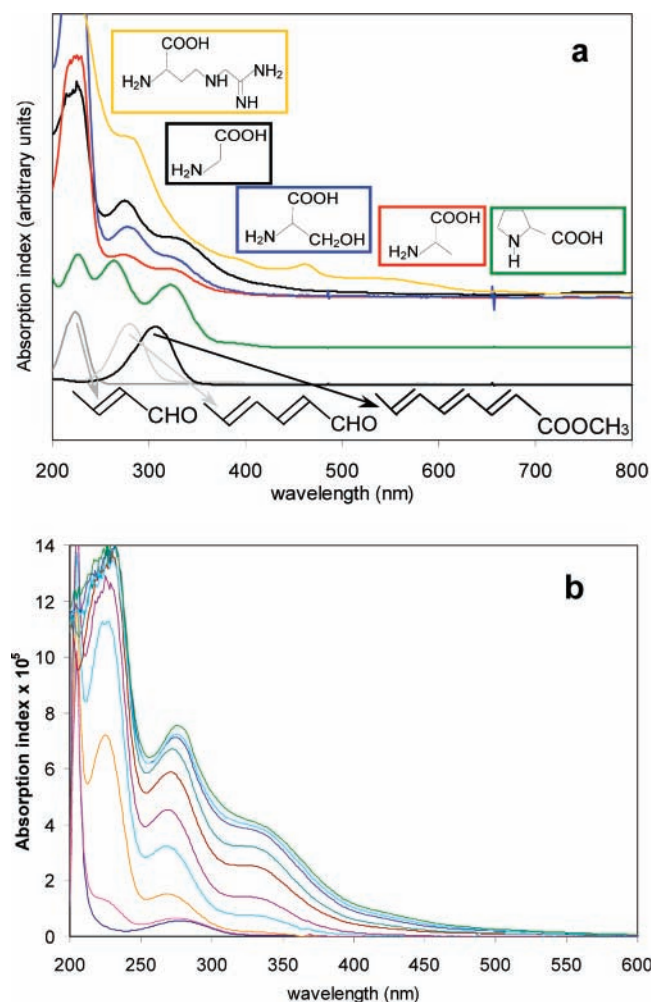


Figure 1. Absorption spectra of reaction mixtures. (a) Reactions catalyzed by glycine (black), serine (blue), alanine (red), proline (green), and arginine (yellow) evidencing the formation of crotonaldehyde (dark gray), 2,4-hexadienal (pale gray), and 2,4,6-octatrienal (black). (b) Evolution of the absorption spectrum over 76 days for the reaction of 0.1 M acetaldehyde catalyzed by 0.06 M glycine in NaCl 4 M.

The present work proposes a kinetic study of amino acid catalyzed aldol condensation reactions with the double objective of obtaining data useful to describe these reactions in the environment and fundamental information on their mechanism. A self-condensation was chosen to clearly distinguish between the C–C bond-forming step and other steps of the mechanism. The reaction of acetaldehyde, chosen as a model for carbonyl compounds, has been studied in water and aqueous salt solutions (NaCl, CaCl₂, Na₂SO₄, MgSO₄). The catalytic efficiency of five of the most abundant amino acids found in atmospheric particles^{7–11} was investigated: glycine, alanine, serine, arginine, and proline. The measurements were based on the formation of three products, crotonaldehyde, 2,4-hexadienal, and 2,4,6-octatrienal, monitored by UV–vis absorption over 200–1100 nm. A first series of experiments focused on determining the overall reaction order in acetaldehyde. A first-order kinetic analysis was then applied to the reactions displaying a first order in acetaldehyde. A third series of experiments focused on the effects of salts on the first-order rate constants. Finally, a last series of experiments studied the kinetics of the reactions displaying a second-order behavior. On the basis of these results, the importance of aldol condensation in natural environments and the general features of its mechanism will be discussed.

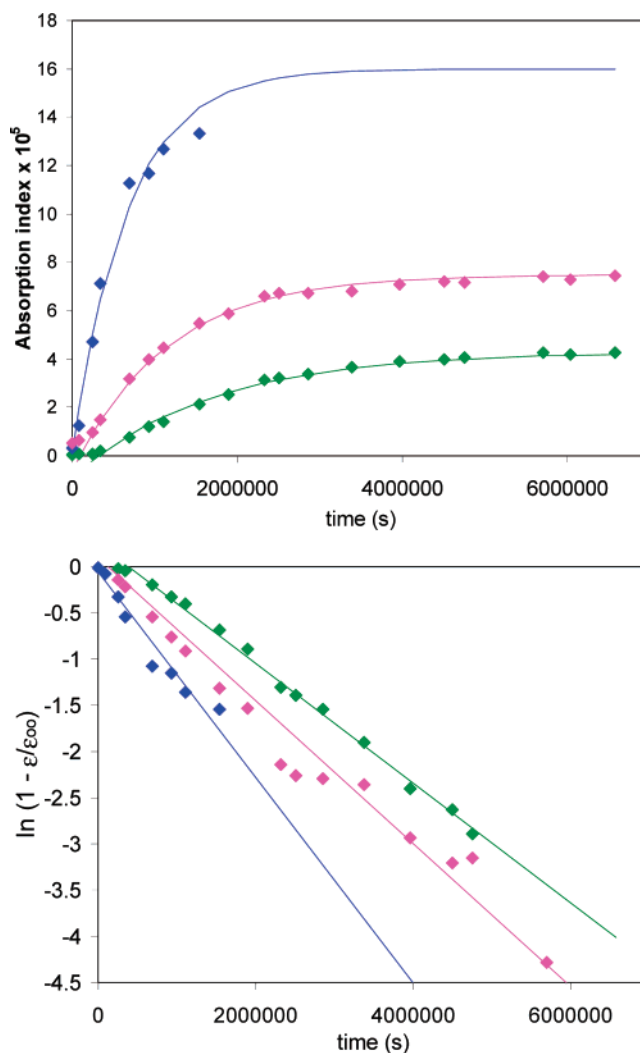


Figure 2. First-order analysis. Top: Real-time variation of the absorption index at 226 nm (blue), 273 nm (pink), and 320 nm (green) for the reaction presented in Figure 1b and first-order fit to eq 3. Bottom: Fit to eq 4 providing the first-order rate constants, k^1 (s⁻¹), for each product.

Experimental Section

The experiments were performed in sealed glass vials and were protected from light with aluminum foil. The vials contained 4 mL of continuously stirred solution at room temperature (295 ± 2 K). The solutions used in this work included deionized water, sodium chloride (NaCl), calcium chloride (CaCl₂), sodium sulfate (Na₂SO₄), and magnesium sulfate (MgSO₄). These solutions were first mixed with 0–0.7 M of different amino acids: glycine, alanine, serine, arginine, and proline. Acetaldehyde (1 mM to 0.5 M) was then introduced with a microsyringe. The kinetic analyses were based on the absorbance of reaction mixtures over 190–1100 nm and were measured with small samples of solutions (<0.3 mL) placed in 1 mm quartz cells and in a UV–vis spectrometer (Agilent 8453). After the measurements, the samples were replaced in the vials. These manipulations accounted for less than 20% of loss on the sample volumes, which represented only small errors on the concentrations.

The absorbance, $A_b(\lambda)$, where λ is the wavelength in centimeters, was measured by the spectrometer and was converted to

TABLE 1: Comparison of the First-Order Rate Constants of Formation of Crotonaldehyde, 2,4-Hexadienal, and 2,4,6-Octatrienal under Various Conditions

[A] ^a (M)	catalyst	[amino acid] (M)	solvent	k_{226}^I (s ⁻¹)	k_{273}^I (s ⁻¹)	k_{320}^I (s ⁻¹)	k_{226}^I/k_{273}^I	k_{273}^I/k_{320}^I
0.1	alanine	0.3	water		5.7×10^{-7}	6.0×10^{-7}		0.9
0.1	glycine	0.06	water	6.3×10^{-7}	2.9×10^{-7}	2.5×10^{-7}	2.2	1.1
0.1	glycine	0.06	NaCl 4 M	1.0×10^{-6}	8.9×10^{-7}	6.5×10^{-7}	1.1	1.4
0.1	glycine	0.06	NaCl 4 M	5.0×10^{-7}	3.0×10^{-7}	2.5×10^{-7}	1.7	1.2
0.1	glycine	0.3	water	4.9×10^{-6}	3.8×10^{-6}	3.4×10^{-6}	1.3	1.1
0.1	glycine	0.2	NaCl 4 M	5.9×10^{-6}	5.5×10^{-6}	5.2×10^{-6}	1.1	1.1
0.1	alanine	0.6	water		2.5×10^{-6}	2.4×10^{-6}		1.1
0.1	serine	0.6	water		2.0×10^{-6}	2.3×10^{-6}		0.9
0.1	glycine	0.3	water	5.5×10^{-6}	3.7×10^{-6}	2.9×10^{-6}	1.5	1.3
0.1	arginine	0.06	water		7.3×10^{-6}	4.9×10^{-6}		1.5
0.1	serine	0.6	NaCl 4 M		3.2×10^{-6}	2.8×10^{-6}		1.2
average							1.5 ± 0.4	1.2 ± 0.2

^a Concentration of acetaldehyde (M).

absorption (or extinction), ϵ_λ , by applying the Beer–Lambert law:

$$A_b(\lambda) = \epsilon_\lambda \times l \quad (1)$$

where l is the optical path length ($l = 0.1$ cm). Because an important application of this work was to determine the effects of the reactions on the optical properties of atmospheric aerosols (as in ref 12), absorption spectra and their time variations are presented in absorption index units in the figures. The relationship between ϵ_λ (cm⁻¹) and the absorption index, A_λ (nondimensional), the imaginary part of the refraction index, is given by

$$A_\lambda = \lambda \times \epsilon_\lambda / 4\pi \quad (2)$$

Since the kinetic analyses were performed at fixed wavelengths (see below), this relationship is a simple multiplicative constant, and this conversion has no implications on the results.

In our recent study,¹² the three main light-absorbing products of the amino acid catalyzed aldol condensation of acetaldehyde in aqueous solutions were identified as crotonaldehyde, 2,4-hexadienal, and 2,4,6-octatrienal by high-resolution mass spectrometry (HRMS) and comparison with the absorption spectra of pure references over 200–1100 nm (Figure 1a). Because 2,4,6-octatrienal was not available, the reference spectrum in Figure 1 is the one of octatrienoic methyl ester. The kinetics of the reactions could not be studied from the decay of acetaldehyde because 2,4-hexadienal absorbs at the same wavelengths and with much larger intensity. Instead, the kinetics was studied from the formation of the light-absorbing products as illustrated in Figure 1b. We will show that, for the reactions studied in this work, both approaches are equivalent. Although the spectra of crotonaldehyde, 2,4-hexadienal, and 2,4,6-octatrienal somewhat overlap, this overlap is minimal at their respective maxima, 226, 273, and 320 nm. These wavelengths were thus chosen for the analyses. Few compounds were expected to interfere with these absorption bands in the experiments. Carbonyl compounds have $n \rightarrow \pi^*$ transition bands in these regions, but those are several orders of magnitudes less intense than the $\pi \rightarrow \pi^*$ bands of the conjugated products (2,4-hexadienal and 2,4,6-octatrienal). This is well illustrated by the small contribution of acetaldehyde to the spectra around 270 nm (bottom spectrum in Figure 1b), which disappeared rapidly and did not interfere with the kinetic analyses. Amino acids contributed to the absorption only below 230 nm as a constant offset (being the catalysts, their concentrations did not vary) and did not affect the kinetic analyses. The only potential interferences to the kinetic analyses that could not be

completely ruled out were the formation of monounsaturated compounds other than crotonaldehyde absorbing below 250 nm. However, such compounds would affect the observed kinetics only if they formed faster or in larger quantities than crotonaldehyde, which was not likely on the basis of the mechanism. Studying the kinetics of the reactions from the absorption of the three light-absorbing products was thus considered reliable. As described below, most determinations of the overall order of reaction in acetaldehyde were performed at these three wavelengths (or two of them). However, determinations of rate constants were mostly performed from the absorption band of 2,4,6-octatrienal at 320 and 350 nm because the latter was the least likely to be subject to spectral interferences and did not reach saturation as fast as those of crotonaldehyde and 2,4-hexadienal.

The kinetic analyses presented in this work were performed on experiments lasting between a few days and 2 months. The results reported in this work are based on over 250 such experiments.

1. Overall Reaction Order in Acetaldehyde. Before determining any rate constant, it was indispensable to establish the overall order of reaction with respect to acetaldehyde. This overall reaction order was determined from the variations of the initial rate of product formation as a function of acetaldehyde concentration. This initial rate was determined from the increase of the absorption of the products, $\Delta\epsilon_\lambda/\Delta t$ (s⁻¹), for up to 25% of conversion (first four to six points in Figure 2). The absolute uncertainties on each value of $\Delta\epsilon_\lambda/\Delta t$ were estimated to be 20% because of the uncertainties in the degree of conversion. However, between values measured in the same series of experiments, the relative uncertainties were only about 15% because the same degree of conversion was chosen even if it was not well-known. In most experiments, the initial acetaldehyde concentration was evaluated precisely by its absorption at 277 nm before product buildup. However, in a few experiments, this concentration could only be estimated from the volume of liquid initially injected because the absorption of acetaldehyde was too small, or its consumption was too fast, which added some uncertainties in the variations of $\Delta\epsilon_\lambda/\Delta t$ (s⁻¹) with acetaldehyde concentration.

2. First-Order Analysis. For the reactions identified as being first-order in acetaldehyde, a first-order analysis was performed to determine the corresponding rate constant, k^I (s⁻¹). The following expression was fitted to the time variations of the absorption, $\epsilon_\lambda(t)$ (see Figure 2a, in absorption index units):

$$\epsilon_\lambda(t) = \epsilon_\infty [1 - \exp(-k^I \times t)] \quad (3)$$

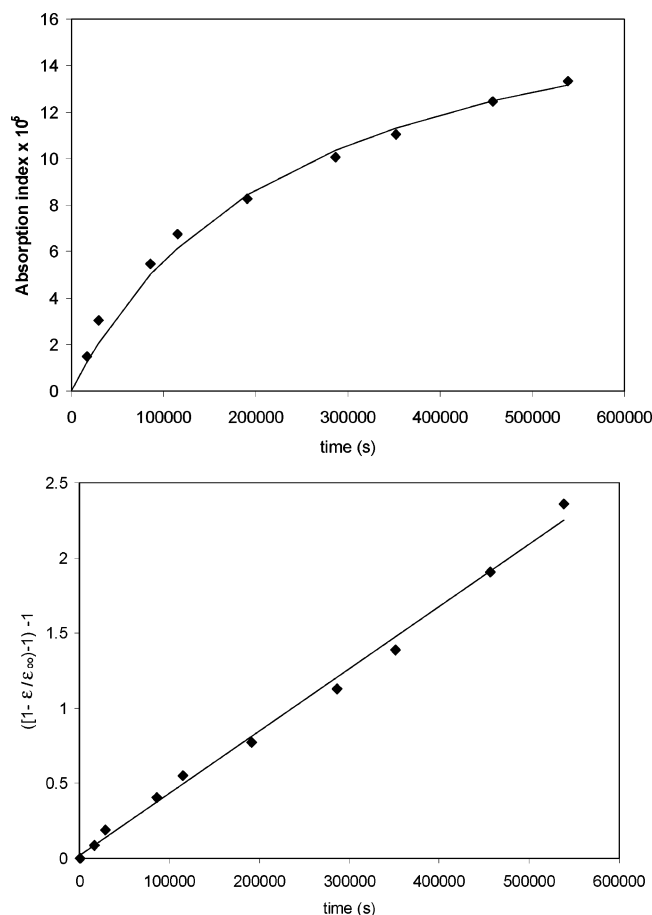


Figure 3. Second-order analysis for the aldol condensation of 0.3 M acetaldehyde catalyzed by arginine in water. Top: Evolution of the absorbance at 350 nm and fit to second-order expression (eq 6). Bottom: Fit to eq 7 to determine the second-order rate constant, k^{II} ($\text{M}^{-1} \text{s}^{-1}$).

where ϵ_{∞} is the absorption of the mixture at long reaction time (or high degree of conversion). All the experiments to which this analysis was applied were carried out until at least 95% conversion. In practice, this degree of conversion was determined as the point at which the absorbance varied by less than 10% (and often randomly), which determined the value of ϵ_{∞} and the uncertainties on it. Depending on the experiment, this was reached after 2 weeks to 2 months during which 10–25 measurements were made. The rate constant, k^{I} (s^{-1}), was determined from the slope of the expression

$$\ln(1 - \epsilon_{\lambda}/\epsilon_{\infty}) = -k^{\text{I}} \times t \quad (4)$$

as illustrated in Figure 2b. Obtaining linear plots from eq 4 was a confirmation that ϵ_{∞} was determined accurately because under- or overestimating this quantity by more than 30% would result in curves upward or downward. Using eq 4 to determine the rate constant also had the important advantage of being independent from the initial concentration of acetaldehyde or the absorption cross sections of the products. The uncertainties on the rate constants obtained from eq 4 were also limited: 10% uncertainties on ϵ_{∞} combined with 5% uncertainties on the measurements of the absorbance, and the errors in the linear regressions resulted in about 25% of uncertainties on k^{I} (s^{-1}). Exceptions were the values of ϵ_{∞} and rate constants determined at 226 nm, which contained many more uncertainties as discussed below.

As illustrated in Figure 2, the formation of the products, especially 2,4-hexadienal and 2,4,6-octatrienal, did not take place immediately but after an induction time, t_0 (s). Such induction times have also been observed in the acid-catalyzed aldol condensation and are due to the time necessary to buildup significant amounts of crotonaldehyde before 2,4-hexadienal and 2,4,6-octatrienal are produced. These induction times did not affect the kinetic analyses or the rate constants since eq 4 can be fitted by replacing t with $(t - t_0)$. However, simulations of the formation of aldol products in natural environments would need to take these induction times into account.

Approximating eq 3 at low reaction conversion gives the expression for the initial rate of product formation, $\Delta\epsilon_{\lambda}^{\text{I}}/\Delta t$ (s^{-1}), measured in the previous series of experiments:

$$\Delta\epsilon_{\lambda}^{\text{I}}/\Delta t \sim \epsilon_{\infty} \times k^{\text{I}} \quad (5)$$

The rate constant k^{I} (s^{-1}) can therefore also be determined from the initial slope $\Delta\epsilon_{\lambda}^{\text{I}}/\Delta t$ and from ϵ_{∞} . This would, however, result in more uncertainties than using eq 4 because the uncertainties on ϵ_{∞} (15%) and $\Delta\epsilon_{\lambda}^{\text{I}}/\Delta t$ (20%) would add up directly, resulting in 35% on k^{I} (s^{-1}). Using eq 4 was thus preferred.

As discussed above, rate constants were generally determined from the absorption of 2,4,6-octatrienal. Potential interferences on this band (from 2,4-hexadienal for instance) were ruled out by obtaining identical rate constants when analyzing the kinetics at two different wavelengths of this band, 320 and 350 nm. Only for the purpose of comparing the rate constants of formation of the three main products were rate constants determined simultaneously at 226, 273, and 320/350 nm (Figure 2 and Table 1).

3. Effect of Salts. Previous works have reported that salts increased the rates of chiral amine catalyzed C–C bond-forming reactions.¹⁶ The possibility of similar effect in the case of amino acid catalysis was investigated in this work by studying the kinetics of the aldol condensation of 0.3 M of acetaldehyde catalyzed by 0.3 M of glycine in aqueous solutions of sodium chloride (NaCl) 0.1–4 M, calcium chloride (CaCl_2) 0.5–2 M, sodium sulfate (Na_2SO_4) 0.5–1 M, and magnesium sulfate (MgSO_4) 0.5–3 M. First, the overall order in acetaldehyde was determined for solutions NaCl 4 M, where the reaction was the fastest and thus most likely to be second-order. Once it was established that this reaction was first-order in these concentrated solutions, and thus in all the salt solutions studied in this work, first-order rate constants were determined in all these solutions using the first-order analysis described above.

4. Second-Order Analysis. As presented below, a second-order kinetics was observed with most amino acids at large amino acid concentrations. This second-order regime was studied with 0.3–0.6 M arginine and an initial concentration of 0.3 M of acetaldehyde. A second-order analysis was applied to the time profiles to determine the second-order rate constant, k^{II} ($\text{M}^{-1} \text{s}^{-1}$). As in the first-order analysis, a time-dependent expression was fitted to the variations of the absorption index at 320 (or 350) nm (Figure 3, top)

$$\epsilon_{320}(t) = \epsilon_{\infty}[1 - 1/(1 + C_{\infty} \times k^{\text{II}} \times t)] \quad (6)$$

where C_{∞} (M) is the concentration of 2,4,6-octatrienal at long reaction time (or high degree of conversion). The second-order rate constant, k^{II} ($\text{M}^{-1} \text{s}^{-1}$), was then obtained from the slope of the expression

$$[1/(1 - \epsilon_{320}/\epsilon_{\infty})] - 1 = C_{\infty} \times k^{\text{II}} \times t \quad (7)$$

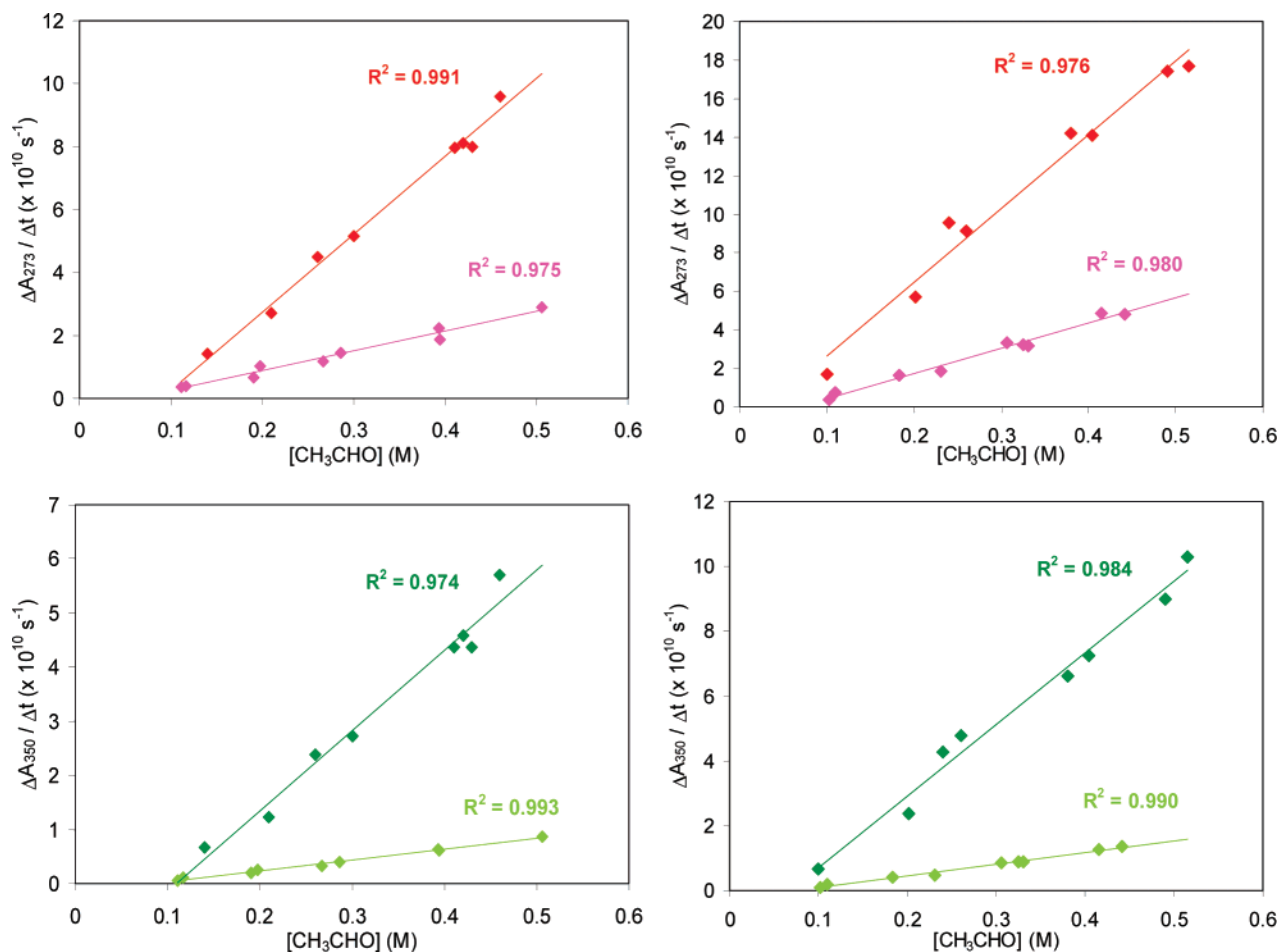


Figure 4. Initial rate of product formation catalyzed by alanine (left column) and serine (right column) evidencing a first-order kinetics in acetaldehyde over the entire range of amino acid concentration studied. Top row: formation of 2,4-hexadienal at 273 nm with 0.3 M (pink) and 0.6 M (red) amino acid; bottom row: formation of 2,4,6-octatrienal at 350 nm with 0.3 M (pale green) and 0.6 M (dark green) amino acid.

(Figure 3, bottom) where C_{∞} was calculated by dividing ϵ_{∞} by the absorption cross section of 2,4,6-octatrienal, $\sigma(320 \text{ nm}) = 37\,150 \text{ M}^{-1} \text{ cm}^{-1}$.¹⁶ Unlike in the first-order analysis, the uncertainties on C_{∞} (assumed identical to those on ϵ_{∞} , 15%) directly reported onto k^{II} ($\text{M}^{-1} \text{ s}^{-1}$) resulting in a total between 35 and 50% of uncertainties.

Approximating eq 6 at low-reaction conversion gives an expression for the initial rate of product formation in the second-order regime

$$\Delta\epsilon_{\lambda}^{\text{II}}/\Delta t \sim \epsilon_{\infty} \times C_{\infty} \times k^{\text{II}} \quad (8)$$

k^{II} ($\text{M}^{-1} \text{ s}^{-1}$) can thus, in principle, also be obtained from these initial formation rates. However, as in the first-order analysis, uncertainties on $\Delta\epsilon_{\lambda}^{\text{II}}/\Delta t$, A_{∞} , and C_{∞} would add up to larger uncertainties than using eq 7.

Chemicals. The solutions were prepared by mixing known quantities of the salts of interest with milliQ water, sodium chloride, calcium chloride, sodium sulfate, and magnesium sulfate: Merck, >99.5%; acetaldehyde, Aldrich, >99.5%; glycine, Aldrich, 99+%; L-alanine and L-serine, Aldrich, 99%; L-proline, Aldrich, 99+%; L-arginine, Aldrich, 98+%; crotonaldehyde, Fluka, >99.5%; 2,4-hexadienal, 95%, Fluka.

Results

1. Overall Reaction Order in Acetaldehyde. The results of the study of the overall reaction order in acetaldehyde are presented in Figures 4 and 5, where values of $\Delta\epsilon_{\lambda}/\Delta t$ are

presented in absorption index units, $\Delta A_{\lambda}/\Delta t$, using the conversion of eq 2. Two distinct kinetic regimes are evident from these results. For alanine and serine at all the concentrations used in this work and for glycine, proline, and arginine at low concentrations (and, for all the amino acids studied, below 0.1 M), the rate of product formation varied linearly with acetaldehyde concentration indicating a first-order kinetics. For larger concentrations of glycine, proline, and arginine (0.3–0.6 M), the rate of product formation varied as the square of the concentration of acetaldehyde evidencing a second-order kinetics. Confidence in these kinetic orders was given by the least-square regression factors, r^2 , which were all larger than 0.8 both for first- and second-order curves. The fact that these regimes took place at different concentrations for different amino acids, and that only one regime was observed with alanine and serine, made it unlikely that these observations resulted from experimental or analytical artifacts.

This transition between kinetic regimes will be discussed in the next section. An important conclusion from these results was that different kinetic analyses had to be performed for different reaction conditions to determine the correct rate constants. These results also showed that, whenever it could be measured, the three products were always in the same kinetic regime (Figures 4 and 5b), which was a first indication that their formation might be limited by the same reaction step.

Another conclusion, more specific to arginine, the only basic amino acid used in this work, is that potential contributions of the base-catalyzed mechanism were likely to be negligible as

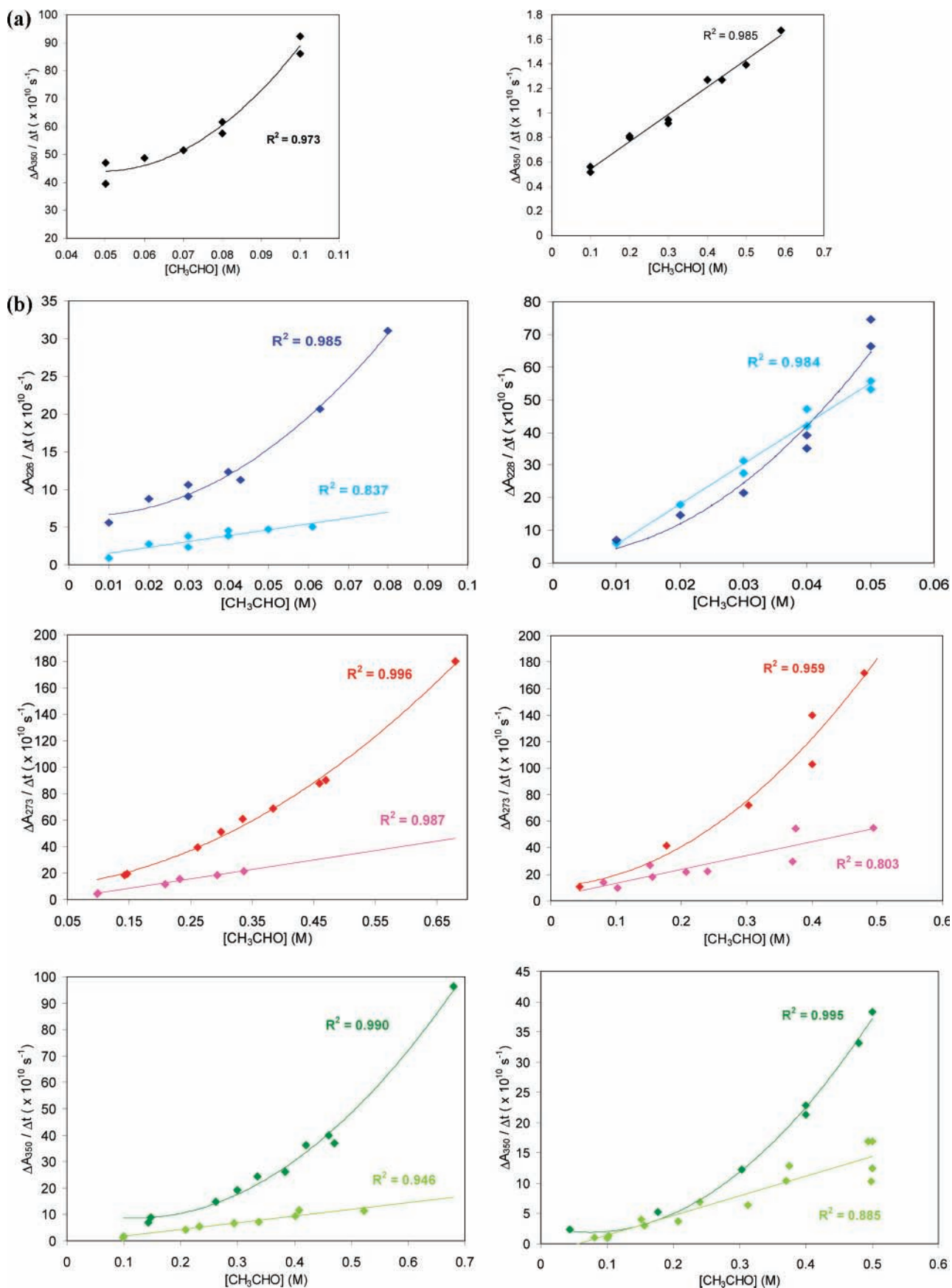


Figure 5. (a) Initial rate of formation of 2,4,6-octatrienal at 350 nm catalyzed by proline (right: 0.1 M; left: 0.6 M) displaying a transition from a first- to a second-order kinetics in acetaldehyde at high amino acid concentration. (b) Rate of product formation showing a transition from a first- to a second-order kinetics for the reaction catalyzed by glycine (left column) and arginine (right column). For glycine: 0.3 M (lines), 0.6 M (curves); for arginine: 0.1 M (lines), 0.3 M (curves): top row: crotonaldehyde measured at 228 nm; middle row: 2,4-hexadienal at 273 nm; bottom row: 2,4,6-octatrienal at 350 nm.

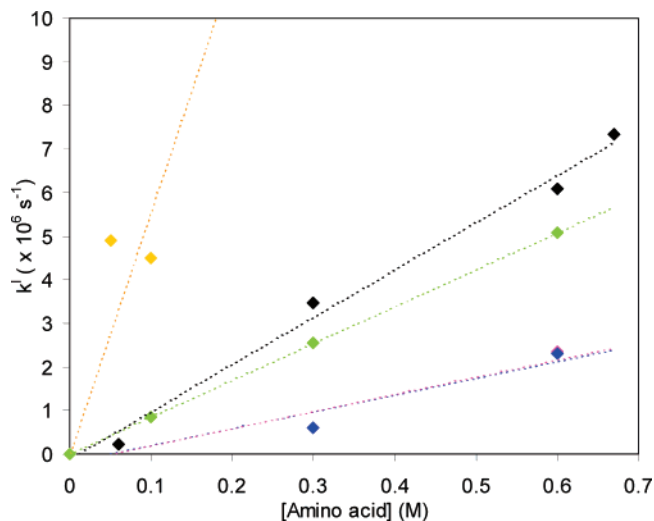


Figure 6. First-order rate constant for the aldol condensation of acetaldehyde in water measured at 320 nm, catalyzed by arginine (yellow), glycine (black), proline (green), serine (blue), and alanine (pink) (data for alanine and serine are almost superimposed).

those should have resulted in a second-order kinetics in acetaldehyde for the whole range of conditions studied.

2. First-Order Kinetics and Effect of Amino Acid Concentration. For a limited number of reactions that were found to be first-order in acetaldehyde, rate constants were determined simultaneously for all three products at 226, 273, and 320 nm (Figure 2). These rate constants and their ratios are presented in Table 1. The errors on the average ratios at the bottom of Table 1 are statistical deviations only. The total uncertainties on the average ratio k_{273}^1/k_{320}^1 were estimated to about 53% (i.e., ± 0.6) when including the 25% uncertainties on k_{273}^1 and k_{320}^1 . The rate constants of formation of 2,4-hexadienal and 2,4,6-octatrienal were thus concluded to be equal. The rate constants measured at 226 nm, k_{226}^1 , contained much larger uncertainties than k_{273}^1 and k_{320}^1 because the absorption band saturated before reaching a high degree of conversion (see Figure 2). It was therefore more difficult to compare the rate constant of formation of crotonaldehyde with those of the two other products. Uncertainties on k_{226}^1 were evaluated to about 50% leading to 75% of uncertainties on the ratios k_{226}^1/k_{273}^1 and a total of 80% on their average, that is, ± 1.2 . Within these large uncertainties, these three rate constants were, however, concluded to be identical. As discussed in the next section, this suggested that the formation of these three products was limited by the same step of the mechanism. Practically, this also meant that determining the kinetics of the adol condensation of acetaldehyde from the consumption of acetaldehyde or from the formation of any of these products should be equivalent.

The first-order rate constants for the reaction in water determined at 320 and 350 nm were also determined at different amino acid concentrations for the five amino acids studied in this work. The results are presented in Figure 6. With arginine, this could only be performed up to 0.1 M beyond which the kinetics became second-order. The rate constants were found to vary linearly with amino acid concentration

$$k_{\text{alanine}}^1 (\text{s}^{-1}) = (3.9 \pm 1.1) \times 10^{-6} \times [\text{alanine}] \quad (9)$$

$$k_{\text{serine}}^1 (\text{s}^{-1}) = (3.8 \pm 1.0) \times 10^{-6} \times [\text{serine}] \quad (10)$$

$$k_{\text{proline}}^1 (\text{s}^{-1}) = (8.5 \pm 2.1) \times 10^{-6} \times [\text{proline}] \quad (11)$$

$$k_{\text{glycine}}^1 (\text{s}^{-1}) = (10.9 \pm 2.1) \times 10^{-6} \times [\text{glycine}] \quad (12)$$

$$k_{\text{arginine}}^1 (\text{s}^{-1}) = (4.5 \pm 1.1) \times 10^{-5} \times [\text{arginine}] \quad (13)$$

where [amino acid] is the molar concentration of amino acid. Uncertainties on eqs 9–13 combine the 25% uncertainties on k^1 from the first-order analysis and 5–12% error in the linear regressions. The slopes of these expressions reflect the relative catalytic efficiency of each amino acid, which was already apparent from the initial rates determined in the first series of experiments: alanine \sim serine $<$ glycine \sim proline $<$ arginine. This is comparable to the relative catalytic efficiencies of the amino acids reported previously for the Michael reaction.^{13a}

3. Effect of Salts on the Kinetics. The reaction catalyzed by 0.3 M of glycine in NaCl 4 M solutions was found to be first-order in acetaldehyde (Figure 7a, in absorption index units). This implied that this reaction would also be first-order in all the salt solutions studied in this work. First-order rate constants were therefore determined for these different solutions using the analysis described above. The results are presented in Figures 7b and 8. The results in Figure 7b show that k^1 displayed linear variations with amino acid concentration in NaCl 4 M, as observed in pure water, but its values were systematically a factor 2 larger. This confirmed our previous observations¹² and earlier works reporting that salts increase the rate of amine-catalyzed reactions.¹⁷ Figure 8 shows that k^1 (s^{-1}) increased linearly with the concentration of dissolved salt in the solutions

$$k_{\text{NaCl}}^1 (\text{s}^{-1}) = (1.1 \pm 0.5) \times 10^{-6} \times [\text{NaCl}] + (3.2 \pm 1.5) \times 10^{-6} \quad (14)$$

$$k_{\text{CaCl}_2}^1 (\text{s}^{-1}) = (2.2 \pm 1.5) \times 10^{-7} \times [\text{CaCl}_2] + (3.2 \pm 1.5) \times 10^{-6} \quad (15)$$

$$k_{\text{Na}_2\text{SO}_4}^1 (\text{s}^{-1}) = (3.1 \pm 1.5) \times 10^{-6} \times [\text{Na}_2\text{SO}_4] + (3.2 \pm 1.5) \times 10^{-6} \quad (16)$$

$$k_{\text{MgSO}_4}^1 (\text{s}^{-1}) = (1.0 \pm 1.5) \times 10^{-6} \times [\text{MgSO}_4] + (3.2 \pm 1.5) \times 10^{-6} \quad (17)$$

where [salt] is the concentration of dissolved salts in solution. The intercept $(3.2 \pm 1.5) \times 10^{-6} \text{ s}^{-1}$, corresponding to the value of k^1 for this reaction in pure water, was imposed to all these expressions. Uncertainties on the slopes combine the 25% uncertainties on each value of k^1 and the errors in the linear regressions. Note that the data with relatively large dispersion in 4 M NaCl shown in Figure 8 are those estimated from initial rates only (presented in Figure 7a) and not from complete first-order analyses, which, as discussed in the Experimental Section, contain larger uncertainties. The results in Figure 8 and eqs 14–17 would, however, benefit from more measurements for a more accurate description of the effects of salts on these reactions.

4. Second-Order Kinetics. The second-order rate constant, k^{II} ($\text{M}^{-1} \text{ s}^{-1}$), obtained from experiments with high concentrations of arginine and eqs 6 and 7 are presented in Figure 9. The variations of k^{II} ($\text{M}^{-1} \text{ s}^{-1}$) with arginine concentration were best

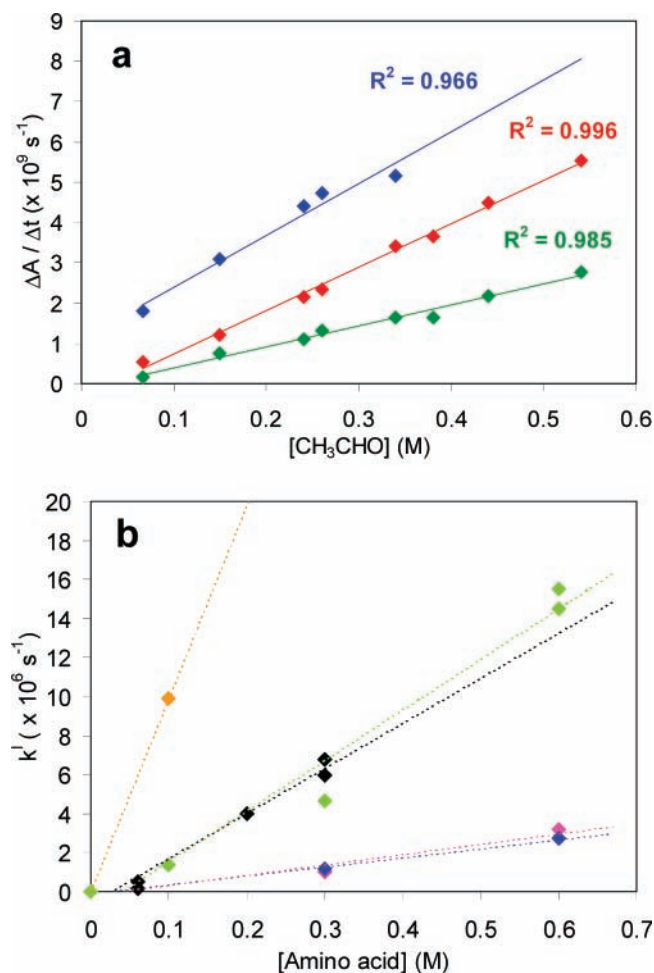


Figure 7. (a) Initial rate of formation of crotonaldehyde (blue), 2,4-hexadienal (red), and 2,4,6-octatrienal (green) for the aldol condensation of acetaldehyde catalyzed by glycine in NaCl 4 M solutions. (b) Variations of the first-order rate constant for the reaction in NaCl 4 M catalyzed by different amino acids. Same colors for the amino acids as in Figure 6.

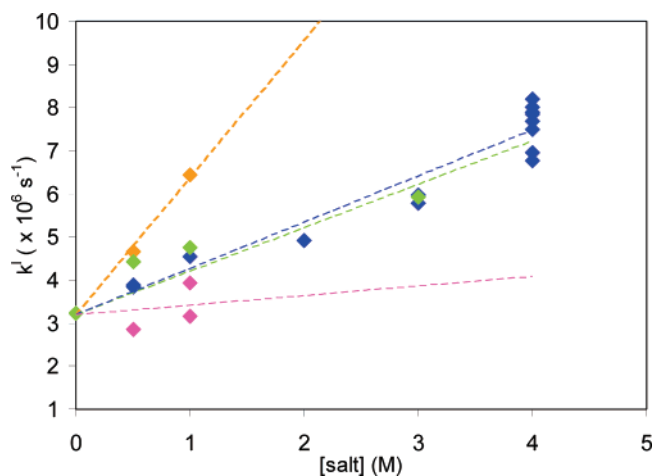


Figure 8. First-order rate constant for the aldol condensation of acetaldehyde catalyzed by 0.3 M glycine in various salt solutions: NaCl (blue), CaCl_2 (pink), Na_2SO_4 (yellow), and MgSO_4 (green).

represented by a second-order expression:

$$k^{\text{II}} (\text{M}^{-1} \text{s}^{-1}) = (8 \pm 4) \times 10^{-2} \times ([\text{AA}] - 0.5)^2 + (6 \pm 3) \times 10^{-3} \quad (18)$$

Overall uncertainties on this expression were estimated to 50%

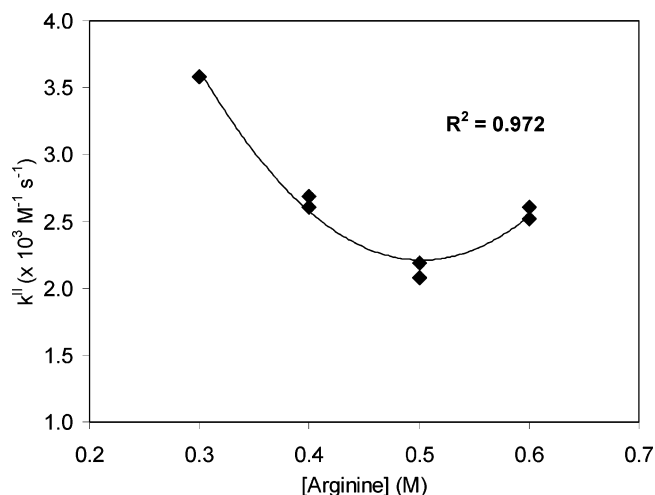


Figure 9. Second-order rate constant for the aldol condensation of acetaldehyde in water at high arginine concentrations.

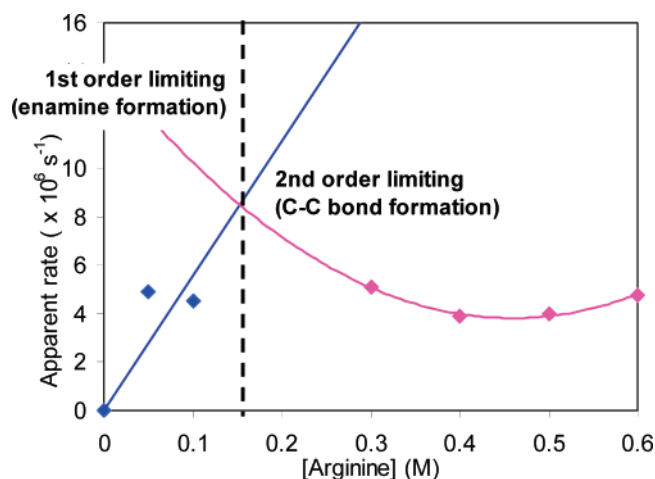


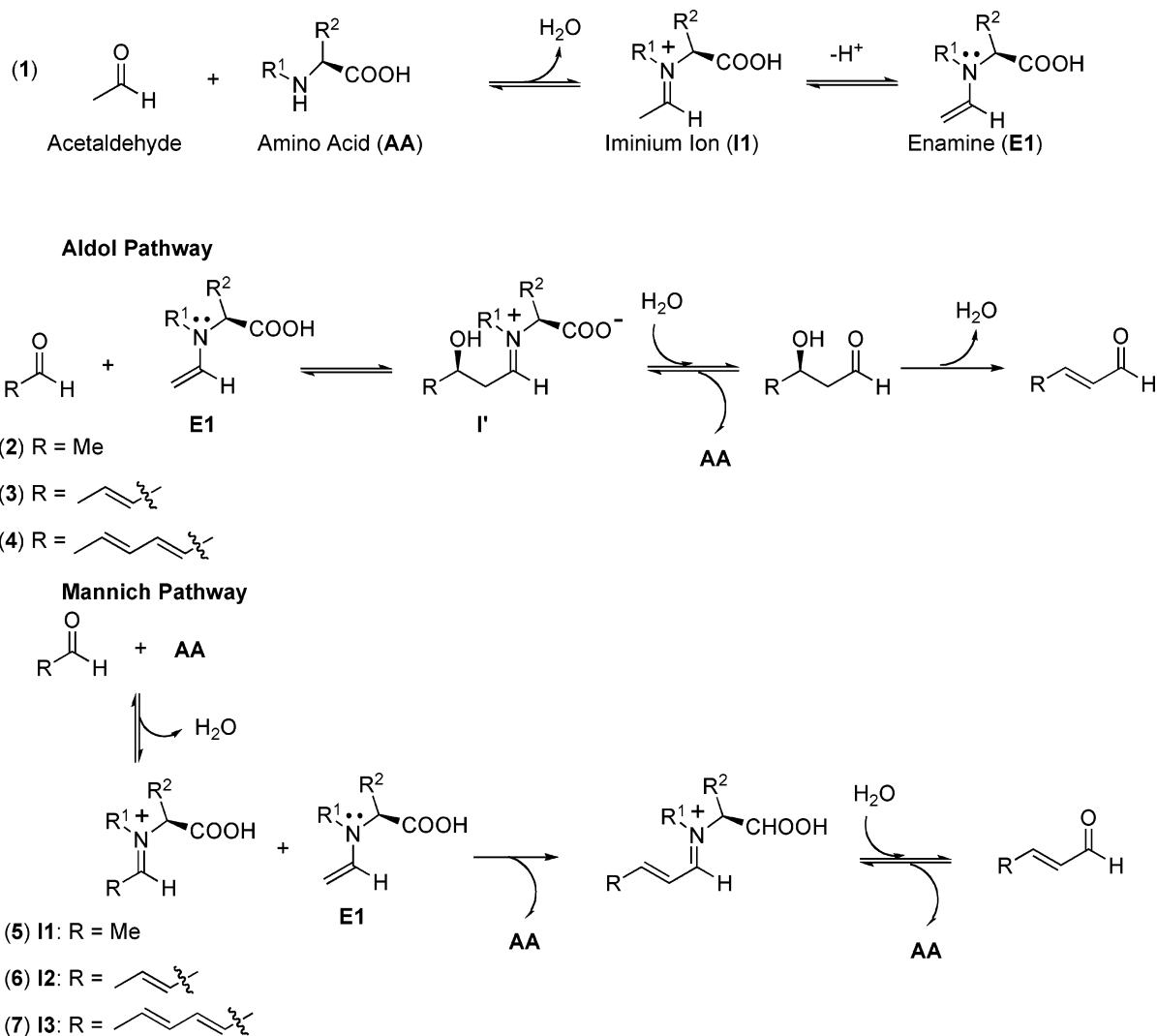
Figure 10. Comparison of the apparent first-order rates for the first- and second-order kinetics for the aldol condensation catalyzed by arginine and determination of the different kinetic regimes.

to reflect the uncertainties on each value of k^{II} ($\text{M}^{-1} \text{s}^{-1}$) and the errors in the second-order regression.

Discussion

A. Mechanism. Competition between Limiting Steps. The transition between the first- and second-order kinetics in acetaldehyde implied that two different steps of the mechanism, one being first-order in acetaldehyde and the other second-order, were in competition to limit the overall reaction speed. This competition is best illustrated by Figure 10 representing the apparent first-order rate constants for the reaction catalyzed by arginine in each regime as a function of arginine concentration. The transition between the two kinetic regimes results from the crossing of these two curves: for $[\text{arginine}] < 0.15 \text{ M}$, the rates corresponding to the first-order curve are smaller than the rates given by the second-order curve and limit the reaction, while above 0.15 M it is the opposite. Figure 10 also explains why this transition occurs at different concentrations for different amino acids: the slope of the first-order line varies proportionally with the catalytic efficiency of each amino acid and, accordingly, intercepts with the second-order curve at different amino acid concentrations. For the least efficient amino acids studied in this work, alanine and serine, the first-order step was slow enough to remain kinetically limiting over the entire range of

SCHEME 1: Main Steps of the Mechanism of the Amino Acid Catalyzed Aldol Condensation of Acetaldehyde



concentrations: the two curves cross at higher amino acid concentrations than studied in this work, and the transition was not observed.

However, for the range of amino acid concentrations around the intercept (for instance, between 0.1 and 0.3 M in Figure 10), there is no clear dominance of one step over the other as both have comparable first-order rates. Therefore, it might not be possible to apply a simple kinetic analysis over this range. This will be further discussed below.

Kinetics and Mechanism of the First-Order Step. The first- and second-order steps controlling the overall kinetics of the amino acid catalyzed aldol condensation will now be identified on the basis of current knowledge of the mechanism. Two different mechanisms, the aldol and Mannich mechanisms, have been proposed for the amino acid catalyzed aldol condensation involving aldehydes as the substrates.^{4f,18} The simplified aldol and Mannich pathways, which possibly both are operating in parallel, are depicted in Scheme 1 for the amino acid catalyzed self-condensation of acetaldehyde. The first step in both pathways is the formation of the enamine intermediate **E1** via the iminium intermediate **I1** (step 1). In the aldol pathway, a nucleophilic attack by the enamine **E1** to the acceptor aldehyde renders the corresponding iminium intermediate **I'**, which upon hydrolysis releases the amino acid and gives the aldol product (step 2). Subsequent dehydration of the aldol product gives crotonaldehyde. This process will be repeated via eqs 3 and 4

to give the corresponding 2,4-hexadienal and 2,4,6-octatrienal. In the Mannich pathway, a nucleophilic attack by the enamine **E1** to the iminium intermediate **I1** gives directly the corresponding iminium ion **I2** after the C–C bond-forming step and elimination of one amino acid molecule (step 5). Thus, two molecules of the amino acid are involved in this step of the reaction. The iminium ion intermediate can either react with another enamine **E1** or upon hydrolysis with water render crotonaldehyde. The former reaction will lead to the formation of the dienal (step 6), which can react further with **E1** to give the corresponding triene (step 6).

In both the aldol and Mannich pathway, the only reaction step that is second-order in acetaldehyde is the C–C bond-forming step, which is step 2 of the aldol pathway and step 5 of the Mannich pathway. The second-order kinetics observed at large concentrations of glycine, proline, and arginine is therefore due to this C–C bond-forming step. By contrast, several steps involve one molecule of acetaldehyde directly or indirectly (i.e., as the enamine **E1**) and could be responsible for the first-order kinetics at low amino acid concentrations: the formation of the enamine **E1** in step 1, the addition of **E1** to crotonaldehyde and 2,4-hexadienal via the aldol pathway in steps 3 and 4, and the formation of the iminium ions from crotonaldehyde and 2,4-hexadienal via the Mannich pathway in steps 6 and 7. However, the results from our experiments suggest that the formation of all three products is kinetically

limited by the same step, which implies that the latter can only be step 1, the formation of iminium ion **II** and enamine **E1**. As a further support to this conclusion, it seems that if neither step 1 nor step 2 were kinetically limiting the reaction, acetaldehyde and crotonaldehyde would be rapidly in equilibrium and all the subsequent steps involving crotonaldehyde (for instance, 3 and 6) would be at least second-order in acetaldehyde, which was not observed.

The linear variations of the first-order rate constant, k^1 (s^{-1}), with amino acid concentration (Figure 6) imply that only one amino acid molecule is involved in the corresponding step, which is also consistent with the mechanism of formation of the enamine **E1** in step 1.

An important conclusion from our results and this discussion is that in natural environments, where amino acid concentrations are much lower than in this work (μM to mM), the aldol condensation of acetaldehyde and, most likely, of other carbonyl compounds should also be controlled by the first enamine formation. Correspondingly, under the conditions employed so far in laboratory to study the amino acid catalyzed aldol condensation (lower concentrations of amino acids than in this work), the C–C bond-forming step could not have been limiting the kinetics. Kinetic and mechanistic information on this C–C bond-forming step could therefore not have been obtained from such experiments and would require concentrations of amino acids of at least 0.3 M.

Effect of Salt. The fact that the aldol condensation of acetaldehyde displays a first-order kinetics in salt solutions (Figure 7a) implies that the formation of the first enamine **E1** (step 1) is also kinetically limiting in these solvents. Therefore, the accelerating effect of the salts is due to an acceleration of the enamine formation. A first possible explanation for this effect could be an electrostatic stabilization of the activated complex between the iminium ion **II** and the enamine **E1** by the solvent (ionic strength effect). In this case, the rate constant should increase proportionally to the ionic strength of the salt and therefore with the same slope in calcium chloride and sodium sulfate solutions. In spite of the uncertainties, our results (Figure 8) show that this is not the case. In fact, ionic strength effects are not expected for intramolecular reactions such as the deprotonation of the iminium ion **II** into the enamine **E1** because the reactant and the activated complex have almost identical charges. If anything, this effect should be slightly negative since the activated complex is slightly less charged than the iminium ion **II**. Another possible explanation for the effect of salts considers the fact that the negative ions of the salts (Cl^- , HSO_4^- , SO_4^{2-}) are weak bases and that the kinetic effect seems correlated with the basicity constants, pK_b , of the salts: water ($pK_b = 17.5$) < $CaCl_2$ ($pK_b = 11.9$)^{19a} < $MgSO_4$ ($pK_b = 9.9$)^{19a} < $NaCl$ ($pK_b = 6.2$)^{19b} < Na_2SO_4 ($pK_b = 5.5$)^{19b} with decreasing value of pK_b indicating stronger bases. The acceleration of the enamine formation could thus result from facilitating the deprotonation of the iminium ion **II** or, alternatively, improving the charge relay system (through deprotonation) of the amino acid to form the iminium ion **II**. This role of the solvent as a weak base would also explain kinetic effects previously observed with organic solvents^{13c} as shown, this time, by their acidity constants, pK_a (increasing value of pK_a indicating stronger bases): water ($pK_a = 15.7$) < isopropanol ($pK_a = 17.1$) < DMSO ($pK_a = 35$) < DMF ($pK_a \sim 40$).

Kinetics and Mechanism of the C–C Bond-Forming Step.

As discussed above, the second-order step can be unambiguously identified as the C–C bond-forming step, since no other step

of the mechanism is second-order in acetaldehyde. Equation 18 obtained for the variations of k^{II} ($M^{-1} s^{-1}$) with amino acid concentration implies that this C–C bond-forming step involves two amino acids and therefore proceeds via the Mannich pathway. However, it cannot be ruled out that this step also contains a first-order component in amino acid (explicit in eq 18) from the aldol pathway. The apparent decrease of the rate constant over 0.3–0.5 M might result from a contribution of the first-order enamine formation step for which a second-order analysis might underestimate the second-order rate constant.

Figure 9 suggests that the second-order Mannich pathway would be dominating above 0.5 M of amino acid and that kinetic investigations of this pathway specifically would require such high concentrations.

B. Environmental Importance. Equations 9–13 allow the calculation of k^1 (s^{-1}) for a wide range of conditions, including natural environments such as atmospheric aerosols. Glycine is usually the most abundant amino acid in atmospheric particles, with a concentration up to 20 pmol m^{-3} (of air) in fine aerosols.^{10,11} Assuming an aerosol specific volume of 10^{-12} (m^3 of aerosol/ m^3 of air), this corresponds to a molar concentration of 20 mM. For this concentration, eq 12 estimates the rate constant in pure water to $k^1 = 1.5 \times 10^{-7} s^{-1}$. Over a typical residence time of the aerosols in the troposphere of 4 days, this rate constant would correspond to a conversion of 15% of the aldehydes initially present in the aerosols into light-absorbing products, which is significant. Other amino acids found in atmospheric particles, although at lower concentrations, would also contribute to catalyze aldol condensation. In particular, only 50 mM of arginine in water resulted in a rate constant of $k^1 = 5 \times 10^{-6} s^{-1}$ in our experiments (Figure 6). This indicates the potential importance of this specific amino acid in natural environments. A more accurate picture of this importance would require further studies below 50 mM of amino acid.

The rate constants reported in this work also allow the first comparison of the catalytic efficiency between amino acids and other catalysts for aldol condensation, such as strong acids: The rate constant estimated above for 20 mM of glycine ($1.5 \times 10^{-7} s^{-1}$) is equivalent to the one measured previously for the same reaction in sulfuric acid 80 wt % (14 M),^{20,21} and the one obtained with 50 mM of arginine in water ($5 \times 10^{-6} s^{-1}$) is equivalent to the rate constant in sulfuric acid 85 wt % (15 M).^{20,21} This clearly illustrates the catalytic efficiency of amino acids.

Conclusion

This work presents a kinetic study of the self-aldol condensation of acetaldehyde catalyzed by different amino acids. For amino acid concentrations lower than 0.1 M in water and salt solutions, the reaction was found to be kinetically limited by the formation of the first enamine, **E1** (step 1). This is therefore likely to be also the case in natural environments and under the laboratory conditions used until now to study these reactions for acetaldehyde and other carbonyl compounds. The rate constant increased linearly with amino acid concentration, in agreement with the enamine formation, which involves a single amino acid molecule. The presence of salts further accelerated enamine formation proportionally to their pK_b either by facilitating the deprotonation of the iminium ion **II** into the enamine **E1** or the formation of the iminium ion **II**. This role of the solvent as a weak base would also explain kinetic effects previously observed with organic solvents.

An important conclusion from this work is that the C–C bond-forming step cannot be kinetically accessed under the

conditions typically used in laboratory to study aldol reactions. This step would become accessible only at high amino acid concentrations (at least 0.3 M) and with efficient amino acids, such as arginine. Our results show that this C–C bond-forming step proceeds through the second-order Mannich pathway but that the contribution of a first-order aldol pathway cannot be ruled out. Investigating specifically the C–C bond-forming step and the Mannich pathway would require at least 0.5 M of amino acid.

With these results, the rate constant for the self-condensation of acetaldehyde catalyzed by 10 mM of amino acids in water and aqueous salt solutions was found to be similar to the one in concentrated sulfuric acid (10–15 M)^{20,21} demonstrating the efficiency of amino acid catalysis. These reactions are therefore likely to be an efficient way for C–C bond formation in aqueous and ionic natural environments.

Acknowledgment. B.N. acknowledges support of a Marie Curie Chair from the European Commission. A.C. acknowledges support from the Swedish National Research Council.

References and Notes

- (1) (a) Fessner, W.-D. In *Stereoselective Biocatalysis*; Patel, R. N., Ed.; Marcel Dekker: New York, 2000, 239. (b) Machajewski, T. D.; Wong, C.-H. *Angew. Chem., Int. Ed.* **2000**, *39*, 1352.
- (2) (a) Trost, B. M.; Fleming, I.; Heathcock, C.-H. *Comprehensive Organic Synthesis*; Pergamon: Oxford, U.K., 1991; Vol. 2. (b) Mukaiyama, T. *Angew. Chem., Int. Ed.* **2004**, *43*, 5590.
- (3) Reviews see: (a) Dalko, P. I.; Moisan, L. *Angew. Chem., Int. Ed.* **2001**, *40*, 3726. (b) List, B. *Tetrahedron* **2002**, *58*, 5573. (c) Duthaler, R. O. *Angew. Chem., Int. Ed.* **2003**, *42*, 975. (d) Dalko, P. I.; Moisan, L. *Angew. Chem., Int. Ed.* **2004**, *43*, 5248. (e) List, B. *Chem. Commun.* **2006**, 819. (f) Berkessel, A.; Gröger, H. *Asymmetric Organocatalysis*; VCH: Weinheim, Germany, 2005.
- (4) For selected references: (a) Hajos, Z. G.; Parrish, D. R. *J. Org. Chem.* **1974**, *39*, 1615. (b) Eder, U.; Sauer, R.; Wiechert, R. *Angew. Chem., Int. Ed.* **1971**, *10*, 496. (c) List, B.; Lerner, R. A.; Barbas, C. F., III. *J. Am. Chem. Soc.* **2000**, *122*, 2395. (d) Notz, W.; List, B. *J. Am. Chem. Soc.* **2000**, *122*, 7386. (e) Sakthivel, K. S.; Notz, W.; Bui, T.; Barbas, C. F., III. *J. Am. Chem. Soc.* **2001**, *123*, 5260. (f) Córdova, A.; Notz, W.; Barbas, C. F., III. *J. Org. Chem.* **2002**, *67*, 301. (g) Northrup, A. B.; MacMillan, D. W. C. *J. Am. Chem. Soc.* **2002**, *124*, 6798. (h) Bøgevig, A.; Kumaragurubaran, N.; Jørgensen, K. A. *Chem. Commun.* **2002**, 620. (i) Tang, Z.; Jiang, F.; Yu, L.-T.; Cui, X.; Gong, L.-Z.; Mi, A.-Q.; Jiang, Y.-Z.; Wu, Y.-D. *J. Am. Chem. Soc.* **2003**, *125*, 5262. (j) Casas, J.; Sundén, H.; Córdova, A. *Tetrahedron Lett.* **2004**, *45*, 7697. (k) Torii, T.; Nakadai, M.; Ishihara, K.; Saito, S.; Yamamoto, H. *Angew. Chem., Int. Ed.* **2004**, *43*, 1983. (l) Córdova, A.; Zou, W.; Ibrahim, I.; Reyes, E.; Engqvist, M.; Liao, W.-W. *Chem. Commun.* **2005**, 3586.
- (5) For selected references see: (a) Brogan, A. P.; Dickerson, T. J.; Janda, K. D. *Angew. Chem., Int. Ed.* **2006**, *45*, 8100. (b) Reymond, J. L.; Chen, Y. *J. Org. Chem.* **1995**, *60*, 6970. (c) Dickerson, T. J.; Janda, K. D. *J. Am. Chem. Soc.* **2000**, *122*, 7386. (d) Córdova, A.; Notz, W.; Barbas, C. F., III. *Chem. Commun.* **2002**, 3024. (e) Chimni, S. S.; Mahajan, D.; Babu, V. V. S. *Tetrahedron Lett.* **2005**, *46*, 5617. (f) Peng, Y.-Y.; Ding, Q.-P.; Li, Z.; Wang, P. G.; Cheng, J.-P. *Tetrahedron Lett.* **2003**, *44*, 3871. (g) Pizzarello, S.; Weber, A. *Science* **2004**, *303*, 1151. (h) Córdova, A.; Ibrahim, I.; Casas, J.; Sundén, H.; Engqvist, M.; Reyes, E. *Chem. Eur. J.* **2005**, *11*, 4772. (i) Mase, N.; Nakai, Y.; Ohara, N.; Yoda, K.; Takabe, K.; Tanaka, F.; Barbas, C. F., III. *J. Am. Chem. Soc.* **2006**, *128*, 734. (j) Dziedzic, P.; Zou, W.; Hafren, J.; Córdova, A. *Org. Biomol. Chem.* **2006**, *4*, 38. (k) Hayashi, Y.; Sumiya, T.; Takahashi, J.; Gotoh, H.; Urushima, T.; Shiji, M. *Angew. Chem., Int. Ed.* **2006**, *45*, 958. (l) Jiang, Z.; Liang, Z.; Wu X.; Lu, Y. *Chem. Commun.* **2006**, 2801.
- (6) Killups, S.; Killops, V. In *Introduction to Organic Geochemistry*; Blackwell Publishing: Oxford, U.K., 2005; p 40.
- (7) Mopper, K.; Zika, R. G. *Nature* **1987**, *325*, 246.
- (8) Milne, P. J.; Zika, R. G. *J. Atmos. Chem.* **1993**, *16*, 361 and references therein.
- (9) Zhang, Q.; Anastasio, C. *Atmos. Environ.* **2001**, *35*, 5629.
- (10) Zhang, Q.; Anastasio, C. *Atmos. Environ.* **2003**, *37*, 2247.
- (11) Matsumoto, K.; Uematsu, M. *Atmos. Environ.* **2005**, *39*, 2163.
- (12) Nozière, B.; Dziedzic, P.; Córdova, A. *Geophys. Res. Lett.* **2007**, *34*, L21812, doi:10.1029/2007GL031300.
- (13) The relative rates of amino acids have also been compared for the Michael reaction; see: (a) Tanaka, F.; Thayumanavan, R.; Barbas, C. F., III. *J. Am. Chem. Soc.* **2003**, *125*, 8523. For investigation of the enamine and iminium ion formation between amines and ketones, see: (b) Hupe, D. J.; Kendall, M. C. R.; Spencer, T. A. *J. Am. Chem. Soc.* **1973**, *95*, 2271. (c) Tanaka, F.; Thayumanavan, R.; Mase, N.; Barbas, C. F., III. *Tetrahedron Lett.* **2004**, *45*, 325.
- (14) Hoang, L.; Bahmanyar, S.; Houk, K. N.; List, B. *J. Am. Chem. Soc.* **2003**, *125*, 16 and references therein.
- (15) (a) Bahmanyar, S.; Houk, K. N. *J. Am. Chem. Soc.* **2001**, *123*, 11273. (b) Bahmanyar, S.; Houk, K. N.; Martin, H. J.; List, B. *J. Am. Chem. Soc.* **2003**, *125*, 2475. (c) Bassan, A.; Zou, W.; Reyes, E.; Himo, F.; Córdova, A. *Angew. Chem., Int. Ed.* **2005**, *44*, 7028. (d) Clemente, F. R.; Houk, K. N. *J. Am. Chem. Soc.* **2005**, *127*, 11294. (e) Gryko, D.; Saletta, W. *J. Org. Biomol. Chem.* **2007**, *5*, 2148.
- (16) Blout, E. R.; Fields, M. *J. Am. Chem. Soc.* **1948**, *70*, 189.
- (17) (a) Mase, N.; Watanabe, K.; Yoda, H.; Takabe, K.; Tanaka, F.; Barbas, C. F., III. *J. Am. Chem. Soc.* **2006**, *128*, 4966. (b) Huang, W.-P.; Chen, J.-R.; Li, X.-Y.; Cao, Y.-J.; Xiao, W.-J. *Can. J. Chem.* **2007**, *85*, 208. (c) Dziedzic, P.; Córdova, A. *Tetrahedron: Asymmetry* **2007**, *18*, 1033. (d) Gryko, D.; Saletta, W. *J. Org. Biomol. Chem.* **2007**, *5*, 2148.
- (18) (a) Hong, B.-C.; Wu, M.-F.; Tseng, H. C.; Liao, J.-H. *Org. Lett.* **2006**, *8*, 2217. (b) Erkkila, A.; Pihko, P. M. *J. Org. Chem.* **2006**, *71*, 2538.
- (19) (a) Approximate values of the p*K*_b's determined in this work by measurement of the ion concentrations in solution by ion chromatography. (b) Hu, W.; Hasebe, K.; Iles, A.; Tanaka, K. *Anal. Sci.* **2001**, *17*, 1401.
- (20) Baigrie, L. M.; Cox, R. A.; Slebocka-Tilk, H.; Tencer, M.; Tidwell, T. T. *J. Am. Chem. Soc.* **1985**, *107*, 3640.
- (21) Esteve, W.; Nozière, B. *J. Phys. Chem. A* **2005**, *109*, 10920.